

Hydrodynamic obstruction to bubble expansion

Thomas Konstandin^a and José M. No^b

^a*CERN Physics Department, Theory Division, CH-1211 Geneva 23, Switzerland*

^b*Institut de Physique Théorique, CEA/Saclay, F-91191 Gif-sur-Yvette Cédex, France*

tkonstan@cern.ch,
jose-miguel.no@cea.fr

Abstract

We discuss a hydrodynamic obstruction to bubble wall acceleration during a cosmological first-order phase transition. The obstruction results from the heating of the plasma in the compression wave in front of the phase transition boundary. We provide a simple criterion for the occurrence of the obstruction at subsonic bubble wall velocity in terms of the critical temperature, the phase transition temperature, and the latent heat of the model under consideration. The criterion serves as a sufficient condition of subsonic bubble wall velocities as required by electroweak baryogenesis.

1 Introduction

Cosmological first-order phase transitions can lead to many interesting phenomena during the evolution of the early universe, such as electroweak baryogenesis [1] or the production of a stochastic background of gravitational waves [2–4]. A first-order phase transition proceeds by bubble nucleation and subsequent bubble expansion and one essential quantity in the description of phenomena linked to the phase transition is the velocity of the expanding bubble walls ξ_w . For example, the electroweak baryogenesis mechanism is based on the diffusion of particle asymmetries into the plasma in front of the bubble wall and subsonic bubble walls are necessary to build up a baryon asymmetry. On the other hand, fast moving walls are essential for the production of a sizable amount of gravitational radiation by bubble collisions [3–7], turbulence [8, 9] or magnetic fields [9].

The analysis of the bubble wall velocity generally assume that after a short period of acceleration of order $\sim 1/T$, (where T represents the typical energy scale associated with the temperature or latent heat of the transition) the pressure difference that drives the bubble expansion is balanced by friction and the bubbles subsequently expand with a constant speed. To quantify this friction requires solving a coupled system of Boltzmann equations for all particle species with a sizable coupling to the Higgs field. This intricate calculation has so far only been performed in the Standard Model (SM) [10] and in the Minimal Supersymmetric Standard Model (MSSM) [11] under the assumption of small wall velocities.

On the other hand, in the limit of highly relativistic wall velocities it is found that the friction in the plasma tends to a constant [12] (up to possible $\log(\gamma_w)$ corrections), opening the possibility of continuously accelerating (runaway) bubble walls when the pressure difference along the phase boundary overcomes this threshold. This runaway behavior is realistic in many models, under the assumption that no hydrodynamic obstruction prohibits that the highly relativistic regime is reached.

The goal of this paper is to analyze one of these possible obstructions based on the heating of the plasma in front of the phase boundary during bubble expansion. Implicitly, this effect was already observed in refs. [10, 13, 14] where finite wall velocities have been reported in the limit of vanishing or at least very small friction. In the recent work [14] this result was obtained under the assumption that the temperature in the Higgs wall is identified with the temperature in front of the phase boundary. Furthermore, the analysis focused on models with an equation of state similar to the standard model. Here, we relax those two assumptions and present a simple criterion for the occurrence of the obstruction. If our criterion holds in a specific model, the wall velocity is subsonic and electroweak baryogenesis is in principle possible. The heating effect only provides an upper limit and a concrete determination of the wall velocity still requires some knowledge of friction. However, as long as friction is not too strong (as it is e.g. the case in the SM) the resulting wall velocities are fairly accurate. Besides, the baryon asymmetry in electroweak baryogenesis is not very sensitive to the wall velocity as long as it is significantly below the speed of sound and large enough to avoid a saturation of the sphaleron process (see e.g. [15] or [16]). Hence, the knowledge of the precise wall velocity is not so relevant for baryogenesis as long as it is subsonic.

The paper is organized as follows: in the next section the hydrodynamic treatment of the system is reviewed, and we briefly sketch the origin of the obstruction. In sec. 3 the heating

effect is discussed analytically in a system with a bag equation of state. We then study how the heating effect impacts the acceleration of the wall in a toy model and present a simple criterion for the occurrence of the obstruction in sec. 4. In sec. 5 we briefly comment on the interplay between the hydrodynamic obstruction and friction before we apply our results to specific models and conclude in sec. 6.

2 Origin of the obstruction

In this section we introduce the basic concepts and set up the notation used for the hydrodynamic analysis of the system of expanding Higgs bubbles [17–19]. For most parts we use the notation of [14].

The dynamics of the combined “wall-plasma” system is determined by the equations of motion of the plasma and of the Higgs field. However, in the present case it is advantageous to replace the equation of motion of the plasma (which would be of Boltzmann type) by the assumption of local thermal equilibrium and energy-momentum conservation, leading to the hydrodynamic approximation. The energy-momentum tensor of the Higgs field ϕ is given by

$$T_{\mu\nu}^{\phi} = \partial_{\mu}\phi\partial_{\nu}\phi - g_{\mu\nu} \left[\frac{1}{2}\partial_{\rho}\phi\partial^{\rho}\phi - V_0(\phi) \right], \quad (1)$$

where $V_0(\phi)$ is the renormalized vacuum potential. If the plasma is locally in equilibrium its energy-momentum tensor can be parametrized as

$$T_{\mu\nu}^{plasma} = w u_{\mu}u_{\nu} - g_{\mu\nu} p, \quad (2)$$

where w and p are the plasma enthalpy and pressure, respectively. The quantity u_{μ} is the four-velocity field of the plasma, related to the three-velocity \mathbf{v} by

$$u_{\mu} = \frac{(1, \mathbf{v})}{\sqrt{1 - \mathbf{v}^2}} = (\gamma, \gamma\mathbf{v}). \quad (3)$$

A constant ϕ background contributes to the total pressure [see eq. (1)] and from now on we will use p for this total pressure, including such contribution. The enthalpy w , the entropy density σ and the energy density e are defined by

$$w \equiv T \frac{\partial p}{\partial T}, \quad \sigma \equiv \frac{\partial p}{\partial T}, \quad e \equiv T \frac{\partial p}{\partial T} - p, \quad (4)$$

where T is the temperature of the plasma. One then has

$$w = e + p. \quad (5)$$

Conservation of energy-momentum is given by

$$\partial^{\mu}T_{\mu\nu} = \partial^{\mu}T_{\mu\nu}^{\phi} + \partial^{\mu}T_{\mu\nu}^{plasma} = 0. \quad (6)$$

We are interested in a system where the bubble expands at a constant speed and, assuming there is no time-dependence, eq. (6) reads in the wall frame (with the wall and fluid velocities aligned in the z direction)

$$\partial_z T^{zz} = \partial_z T^{z0} = 0. \quad (7)$$

Integrating these equations across the phase boundary and denoting the phases in front and behind the wall by subscripts $+$ (symmetric phase) and $-$ (broken phase) one obtains the matching equations (in the wall frame):

$$w_+ v_+^2 \gamma_+^2 + p_+ = w_- v_-^2 \gamma_-^2 + p_- , \quad w_+ v_+ \gamma_+^2 = w_- v_- \gamma_-^2 . \quad (8)$$

From these equations we can obtain the relations [18]

$$v_+ v_- = \frac{p_+ - p_-}{e_+ - e_-} , \quad \frac{v_+}{v_-} = \frac{e_- + p_+}{e_+ + p_-} . \quad (9)$$

In a concrete model the thermodynamic potentials can be calculated in the two phases and the temperature at which the phase transition happens can be determined using the standard techniques [21]. Still, there are three unknown quantities (T_- , v_+ and v_-) and only two equations (9), so that up to this point all hydrodynamically viable solutions are parametrized by one parameter. We will parametrize the solution by its wall velocity ξ_w .

Ultimately, the wall velocity is deduced from the equation of motion of the Higgs

$$\square\phi + \frac{\partial V_0}{\partial\phi} + \sum_i \frac{dm_i^2}{d\phi} \int \frac{d^3p}{(2\pi)^3 2E_i} f_i(p) = 0 , \quad (10)$$

where f_i denotes the particle distribution function of the i th species. By decomposing

$$f_i(p) = f_i^{eq}(p) + \delta f_i(p) , \quad (11)$$

where $f_i^{eq} = 1/[\exp(E_i/T) \mp 1]$ is the equilibrium distribution function with $E_i^2 = p^2 + m_i^2$, eq. (10) takes the simple form

$$\square\phi + \frac{\partial\mathcal{F}}{\partial\phi} - \mathcal{K}(\phi) = 0 . \quad (12)$$

The second term contains the free energy \mathcal{F} that drives the expansion of the bubble and $\mathcal{K}(\phi)$ stands for the friction term that arises from deviations of the particle distributions in the plasma from equilibrium. In principle, calculation of $\mathcal{K}(\phi)$ involves solving a coupled system of Boltzmann equations for all particle species with a sizable coupling to the Higgs field. This intricate calculation has been performed in the Standard Model [10] and in the MSSM [11] and under the assumption that the deviation from thermal equilibrium is small, i.e. $\delta f_i(p) \ll f_i(p)$, which is only true for weakly first-order phase transitions.

The aim of the present work is to show that the bubble wall velocity can approach a subsonic value even if the friction is very small - contrary to the naive expectation of supersonic velocities or even runaway behavior in the limit of very small friction. The occurrence of this effect can be understood by inspecting eq. (12). Assuming that in the steady state the bubble is large enough so that one can use the planar limit, one obtains by integration the pressure (in the wall frame) that drives the expansion

$$F_{dr} = \int dz \partial_z \phi \frac{\partial\mathcal{F}}{\partial\phi} = \int dz \partial_z \phi \mathcal{K} = F_{fr} . \quad (13)$$

The physical interpretation of this equation is that the change of pressure in the wall drives the expansion of the bubble and this driving force F_{dr} is ultimately balanced by the friction

force F_{fr} in order to reach a stationary state. Without the influence of the bubble, this change in pressure is always positive, since nucleation requires the temperature in the symmetric phase to be below the critical one. However, some particles are reflected at the phase boundary, leading to a heating effect in front of the wall. Hence the temperature experienced by the phase boundary is increased and a hydrodynamic obstruction can occur when the bubbles accelerate while building up a compression wave in front of the Higgs wall. At some velocity, the average temperature¹ in the wall might approach the critical one, the driving force goes to zero and the bubble cannot further accelerate even in the limit of vanishing friction as defined by (12) and (13).

As a final remark in this section, notice that there is a certain freedom in splitting the last term of (10) into equilibrium and friction contributions. At the critical temperature T_c (where the pressure in the two phases is equal), the only solution to (12) is a static wall. The plasma is at rest and the temperatures on both sides of the Higgs wall coincide: the system is in equilibrium everywhere. For a temperature below the critical one, all deviations from equilibrium in the particle distributions are proportional to the wall velocity and also the friction term vanishes in the limit of zero velocity. This leaves a certain arbitrariness in the temperature profile of the equilibrium distributions f_i^{eq} in (11) along the wall and different choices for the temperature profile in the equilibrium distributions will result in different friction terms.

A necessary feature of the temperature profile is that it interpolates between the two values T_+ and T_- . This ensures that the deviations from equilibrium δf_i vanish away from the bubble wall. Besides, an upper bound on the wall velocity will be derived in the following by neglecting the friction term. Hence, one has to ensure that the friction term is always positive and reduces the wall velocity for the chosen temperature profile. A very convenient choice for the temperature profile is obtained by enforcing conservation of the two energy-momentum tensors resulting from the particle distributions f_i^{eq} and δf_i separately. First, this has the advantage that in the limit of infinite interaction rates the particle distribution functions f_i^{eq} are the physical ones and δf_i will vanish. Second, for this choice entropy is conserved when the deviations δf_i are neglected. A simple phenomenological approach for the friction term shows (see e.g. ref. [22]) that negative friction terms would lead to entropy decrease. This indicates that in general the H-theorem ensures that the expansion around this equilibrium leads to positive friction terms that reduce the wall velocity. We will essentially utilize this choice for the temperature profile in section 4.

3 The heating effect

In this section we discuss a system whose equation of state is in the broken phase given by

$$p_- = \frac{1}{3}a_-T_-^4 + \epsilon, \quad e_- = a_-T_-^4 - \epsilon, \quad (14)$$

where ϵ denotes the false-vacuum energy resulting from the Higgs potential, while in the symmetric phase

$$p_+ = \frac{1}{3}a_+T_+^4, \quad e_+ = a_+T_+^4, \quad (15)$$

¹We will be more specific what the average temperature is in sec. 4.

with a different number of light degrees of freedom across the wall and therefore different values a_+ and a_- (with $a_+ > a_-$) and different temperatures on both sides of the wall. These expressions correspond to the so-called bag equation of state. This approximation works reasonably well when the Higgs vev does not change much in between the critical temperature and zero temperature and particles can be independently of the temperature divided into “light” and “heavy” in the two phases. In particular, this is the case for models where the potential barrier between the broken and symmetric phases is present even at vanishing temperature, generally leading to relatively strong phase transitions.

For temperatures close to the critical one, it is more physical to parametrize the pressure and energy density in the symmetric and broken phases by

$$p_- \simeq \frac{1}{3}a_+T_-^4 - \ell_c(T_-/T_c - 1), \quad p_+ \simeq \frac{1}{3}a_+T_+^4, \quad (16)$$

$$e_- \simeq a_+T_-^4 - \ell_c, \quad e_+ \simeq a_+T_+^4, \quad (17)$$

and ℓ_c is the latent heat at the critical temperature. Comparing with the bag equation of state one can identify

$$\ell_c = \frac{4}{3}(a_+ - a_-)T_c^4 = 4\epsilon. \quad (18)$$

Our analysis will be done mostly assuming the bag equation of state in order to facilitate comparison with the existing literature. However, when rephrased in terms of the latent heat all results are equally applicable to models with a weak phase transition where the bag equation of state does not hold.

Using the bag equations of state (14) and (15) in eq. (9) we get

$$\begin{aligned} v_+v_- &= \frac{1 - (1 - 3\alpha_+)r}{3 - 3(1 + \alpha_+)r}, \\ \frac{v_+}{v_-} &= \frac{3 + (1 - 3\alpha_+)r}{1 + 3(1 + \alpha_+)r}, \end{aligned} \quad (19)$$

where we defined

$$\alpha_+ \equiv \frac{\epsilon}{a_+T_+^4} = \frac{\ell_c}{4a_+T_+^4}, \quad r \equiv \frac{a_+T_+^4}{a_-T_-^4}. \quad (20)$$

The quantity α_+ is the ratio of the vacuum energy to the radiation energy density and typically characterizes the “strength” of the phase transition: the larger α_+ the stronger the phase transition. These two equations can be combined to give

$$v_+ = \frac{1}{1 + \alpha_+} \left[\left(\frac{v_-}{2} + \frac{1}{6v_-} \right) \pm \sqrt{\left(\frac{v_-}{2} + \frac{1}{6v_-} \right)^2 + \alpha_+^2 + \frac{2}{3}\alpha_+ - \frac{1}{3}} \right], \quad (21)$$

so that there are two branches of solutions, corresponding to the \pm signs in eq. (21).

Generally, there are three different types of solutions for the bulk fluid motion (recent reviews on the topic can be found in [14] and [20]): Detonations, deflagrations and hybrid solutions. In detonations, the wall expands at supersonic velocities and the vacuum energy of the Higgs leads to a rarefaction wave behind the bubble wall, while the plasma in front of

the wall is at rest. In this case, the wall velocity is $\xi_w = v_+ > v_-$, and therefore detonations are identified with the + branch of solutions in (21). In deflagrations, the plasma is mostly affected by reflection of particles at the bubble wall and a compression wave builds up in front of the wall while the plasma behind the wall is at rest. In this case, the wall velocity is identified with $\xi_w = v_- > v_+$, corresponding to the - branch of solutions in (21). “Pure” deflagrations are subsonic, while the hybrid case occurs for supersonic deflagrations where both effects (compression and rarefaction wave) are present. In the following we are concerned with deflagrations.

In the following we present a rough constraint for the occurrence of the obstruction. We assume that the bag equation of state holds even locally in the wall such that the pressure is given by the simple expression $p = \frac{1}{3}a(\phi)T^4$. Then, the driving force (13) reads

$$F_{dr} = \int dz \partial_z \phi \frac{\partial \mathcal{F}}{\partial \phi} = \epsilon - \frac{1}{3} \int da T^4 . \quad (22)$$

For a monotonously changing temperature in the wall, the last contribution is bounded by (we will see later on that $T_- < T_+$)

$$\frac{1}{3}(a_+ - a_-)T_-^4 < \epsilon - F_{dr} < \frac{1}{3}(a_+ - a_-)T_+^4 . \quad (23)$$

Analogously to α_+ one can define the quantities α_N , α_- and α_c as the vacuum energy normalized to the energy density in the symmetric phase, behind the wall and at the critical temperature

$$\alpha_- = \frac{\epsilon}{a_- T_-^4} , \quad \alpha_N = \frac{\epsilon}{a_+ T_N^4} , \quad (24)$$

$$\alpha_c = \frac{\epsilon}{a_+ T_c^4} = \frac{1}{3} \frac{a_+ - a_-}{a_+} < \frac{1}{3} . \quad (25)$$

The nucleation of bubbles happens at temperatures below the critical one, $\alpha_c < \alpha_N$. After nucleation, the bubble wall accelerates, increasing T_+ and therefore decreasing α_+ . Likewise, T_- is expected to increase and α_- to decrease during the acceleration. If the phase transition is sufficiently weak, this heating effect eventually leads to a vanishing driving force and the acceleration of the wall ceases. According to (23) this has to happen somewhere in the window

$$T_- < T_c < T_+ . \quad (26)$$

We will show that for small wall velocities the relation $T_+ > T_- > T_N$ holds, so the hydrodynamic obstruction definitely occurs in models where T_N is very close to T_c .

In the following we briefly review the solutions of the plasma velocity in the limit of small wall velocities ξ_w as done in [14]. For deflagrations, the fluid in the bubble is at rest and changes in the bubble wall to a finite value according to (21) where v_- is identified with the wall velocity ξ_w . The fluid motion in the compression wave is then determined by hydrodynamics. Since there is no intrinsic macroscopic length scale present in the system, solutions to the hydrodynamic equations are self-similar and only depend on the combination $\xi = r/t$, where r denotes the radial coordinate of the bubble and t the time since nucleation. The plasma then fulfills the equations

$$2 \frac{v}{\xi} = \gamma^2 (1 - v\xi) \left[\frac{\mu^2}{c_s^2} - 1 \right] \partial_\xi v , \quad (27)$$

and

$$\frac{\partial_\xi w}{w} = 4\gamma^2 \mu(\xi, v) \partial_\xi v , \quad (28)$$

where $c_s = 1/\sqrt{3}$ denotes the velocity of sound in the plasma and $\mu(\xi, v)$ is the Lorentz-transformed fluid velocity

$$\mu(\xi, v) = \frac{\xi - v}{1 - \xi v} . \quad (29)$$

An example of the fluid motion and the enthalpy in case of a deflagration is shown in Fig. 1.

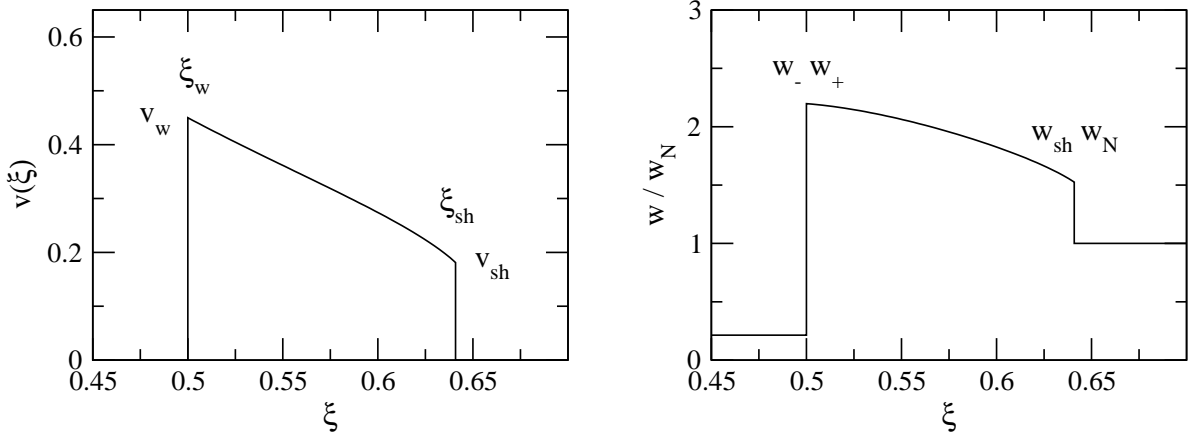


Figure 1: Example for a deflagration. The left plot shows the fluid velocity $v(\xi)$ while the right plot shows the enthalpy $w(\xi)$.

The boundary conditions for deflagrations read in the rest frame

$$v_w \equiv v(\xi_w) = \mu(v_-, v_+) , \quad (30)$$

and the fluid velocity in the compression wave is for small wall and fluid velocity ($\xi_w, v \ll 1$) given by

$$v(\xi) \simeq v_w \frac{\xi_w^2}{\xi^2} , \quad \xi \in [\xi_w, c_s] . \quad (31)$$

The enthalpy changes in the compression wave between the Higgs wall and the plasma in front of the shock by a factor (there is also a jump in the enthalpy in the shock front which is however of order ξ_w^3)

$$\frac{T_+^4}{T_N^4} = \frac{\alpha_N}{\alpha_+} = \frac{w_+}{w_N} \simeq \exp \left[4 \int_{v(c_s)}^{v(\xi_w)} \mu(\xi, v) dv \right] \approx \exp(8 \xi_w v_w) . \quad (32)$$

So in this limit indeed $T_+ > T_N$, as required for an obstruction (26). Using the bag equation of state and (21) one finds

$$\frac{v_+}{v_-} \simeq 1 - 3\alpha_+ - 6\alpha_+ \xi_w^2 , \quad (33)$$

and hence

$$v_w \approx 3\alpha_+ \xi_w . \quad (34)$$

If the obstruction would occur as soon as T_+ exceeds the critical temperature, the wall velocity would be

$$\xi_w^2 = \frac{\log \frac{T_c}{T_N}}{6\alpha_c} . \quad (35)$$

Nevertheless, T_- is typically smaller than T_+ , so a more conservative bound arises from the pressure in the broken phase, that is determined using

$$\frac{w_+}{w_-} = \frac{v_- \gamma_-^2}{v_+ \gamma_+^2} \approx \frac{1 + 12\alpha_+ \xi_w^2}{1 - 3\alpha_+} , \quad (36)$$

such that

$$\frac{T_+^4}{T_-^4} = \frac{a_- w_+}{a_+ w_-} = \frac{1 - 3\alpha_c}{1 - 3\alpha_+} (1 + 12\alpha_+ \xi_w^2) \simeq 1 + 12\alpha_+ \xi_w^2 , \quad (37)$$

and hence (using (32))

$$\log \frac{T_-}{T_N} \simeq 3\xi_w^2 \alpha_+ . \quad (38)$$

Assuming that the obstruction occurs for $T_- = T_c$ one finds analogously to (35) (assuming $\alpha_c \simeq \alpha_+$ in a first approximation)

$$\xi_w^2 = \frac{\log \frac{T_c}{T_N}}{3\alpha_c} , \quad (39)$$

and hence a slightly larger wall velocity. The obstruction should hence be somewhere in the range

$$\xi_w^2 \in (3 \pm 1) \frac{1}{12} \frac{\log \frac{T_c}{T_N}}{\alpha_c} . \quad (40)$$

However, even if this criterion leads to a supersonic wall velocity, the obstruction might still be present, since for sizable wall velocities the above approximation underestimates the effect of the heating. In order to show this last statement, we assume a large but subsonic wall velocity $\xi_w \lesssim c_s$. When the wall velocity becomes supersonic, the expansion mode by deflagration is prone to decay into a detonation and we assume that the obstruction is absent in this case [13]. In the following we derive some analytic results under the assumption $\alpha_+ \ll 1$ and then present some numerical results for $\xi_w = c_s$ and arbitrary α_+ . In this case we obtain for the plasma velocity in front of the wall (using (21))

$$v_+ \simeq c_s \frac{1 - \sqrt{\alpha_+(2 + 3\alpha_+)}}{1 + \alpha_+} + O((\xi_w - c_s)^2) . \quad (41)$$

Notice that positive velocities imply that $\alpha_+ < 1/3$. If α_+ is larger than this value, deflagrations are not possible and the bubble expansion proceeds by supersonic detonations. In the wall frame the plasma has in front of the wall the velocity

$$v_w = \mu(\xi_w, v_+) \simeq \frac{3}{2} \left((\xi_w - c_s) + \sqrt{2\alpha_+/3} \right) , \quad (42)$$

which is obviously only a valid approximation for $(c_s - \xi_w) \lesssim \sqrt{2\alpha_+/3}$. Comparing (34) with (42) shows that for wall velocities close to the speed of sound the heating effect in front of the wall is much more efficient than in the limit of small wall velocities. The bound (40) is hence a conservative one.

In the compression wave the plasma velocity decreases to a value v_{sh} and then drops to zero in the shock front. The decrease in enthalpy in the compression wave is of order (using (28))

$$\log \frac{T_+}{T_{sh}} \simeq c_s(v_w - v_{sh}) + O(v_w^2, v_{sh}^2) , \quad (43)$$

whereas the jump in enthalpy in the shock front is of order (using (8) in the shock front)

$$\frac{T_{sh}^4}{T_N^4} \simeq \exp(4c_s v_{sh}) + O(v_{sh}^3) . \quad (44)$$

We therefore obtain

$$\log \frac{T_+}{T_N} \simeq c_s v_w \simeq \frac{3}{2} c_s \left((\xi_w - c_s) + \sqrt{2\alpha_+/3} \right) , \quad (45)$$

which is in leading order independent of the value of the fluid velocity at the shock front v_{sh} and the fluid profile in the compression wave.

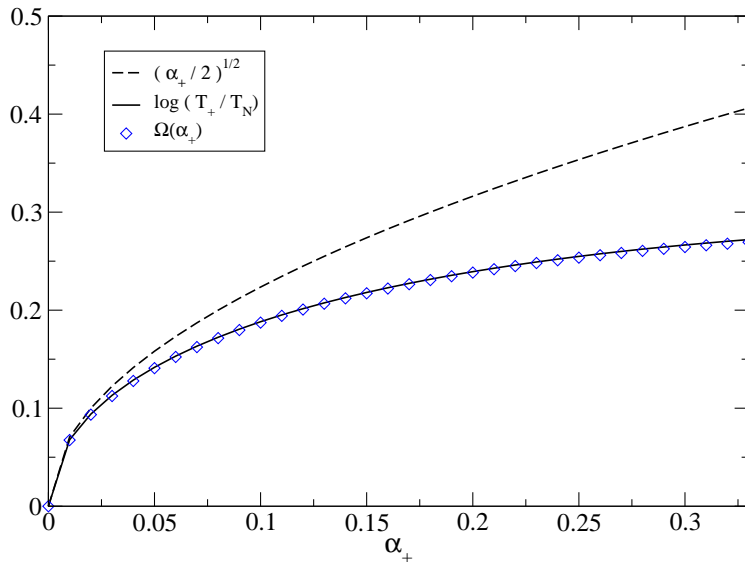


Figure 2: The heating effect assuming a wall velocity of the speed of sound, $\xi_w = c_s$. The plot shows $\log T_+/T_N$ as a function α_+ . The dashed line is the leading order result (46) while the straight line is the fit (47) to the numerical result.

To derive a simple criterion for the occurrence of the obstruction, we assume again that the average temperature in the wall is close to T_+ and that supersonic deflagrations can decay into detonations. For a fixed value of α_+ , one can then determine from (45) in leading order in α_+

$$\log \frac{T_+}{T_N} \simeq \sqrt{\alpha_+/2} . \quad (\xi_w = c_s) \quad (46)$$

The full numerical result is shown in Fig. 2, and a formidable fit is given by

$$\log \frac{T_+}{T_N} \simeq \sqrt{\alpha_+/2} - \frac{3}{10}\alpha_+ - \frac{1}{5}\alpha_+^{3/2} \equiv \Omega(\alpha_+) . \quad (\xi_w = c_s) \quad (47)$$

If the obstruction would occur as soon as the temperature in front of the wall T_+ surpasses the critical temperature T_c , an easy and model independent criterion for the occurrence of the obstruction would be

$$\log \frac{T_c}{T_N} < \Omega(\alpha_c) . \quad (48)$$

However, the enthalpy in the bubble interior is in leading order (which is $O(\sqrt{\alpha})$) given by

$$w_- \approx (1 - 4c_s v_w)w_+ \approx w_N , \quad (49)$$

and so the temperature in the bubble is close to the nucleation temperature. In the limit $\alpha_c \rightarrow 1/3$, the temperature behind the wall even vanishes. Hence, one expects that the temperature T_+ has to surpass the critical temperature T_c significantly to obtain an average temperature in the wall that is close to the critical one. To obtain the wall velocity corresponding to the hydrodynamic obstruction (if present) requires the knowledge of the temperature profile in the wall in order to determine the average temperature experienced by the Higgs. This is the topic of the next section.

4 Local equations of motion in a toy model

In the last section, we presented results for the heating effect in front of the wall during the bubble expansion. In particular, we exemplified how to calculate the temperature on both sides of the Higgs wall, T_+ and T_- , as functions of the wall velocity ξ_w , the strength of the phase transition α_+ and the nucleation temperature T_N . The topic of the present section is to connect this heating effect with the occurrence of the obstruction to bubble acceleration. An exact treatment of this question would require to determine the particle distribution functions by solving a system of Boltzmann equations. The thermodynamic potentials in the wall could then be obtained via (10). On the other hand, the obstruction has to happen in the window given by eq. (26) and any simplifying assumption should lead to reasonable bubble wall velocities. In this section, we assume that the ansatz of local equilibrium (2) also applies in the bubble wall. This approximation becomes exact in the limit that the mean free path of the particles in the plasma is much shorter than the bubble wall thickness. Even though the mean free path of some particles is much larger than the wall thickness, we expect that the free energy should not depend too much on the out-of-equilibrium features of the particle distribution functions since energy-momentum conservation generally holds (see also the comments at the end of section 2).

4.1 Solving the local equations of motion

To obtain the steady-state profiles across the phase transition wall of quantities like the velocity, temperature and Higgs field, we integrate the following system of coupled differential

equations in the planar limit:

$$\partial_z^2 \phi + \frac{\partial p}{\partial \phi} - \mathcal{K} = 0 , \quad (50)$$

$$\partial_z [\omega \gamma^2 v] = 0 , \quad (51)$$

$$\partial_z \left[\frac{1}{2} (\partial_z \phi)^2 + \omega \gamma^2 v^2 + p \right] = 0 . \quad (52)$$

The first equation is the Higgs equation (12) and to be specific we use the friction term (see [14] and also [23] for a similar approach)

$$\mathcal{K} = -T_N \eta v \partial_z \phi . \quad (53)$$

The particular form of the friction term is not relevant since we are interested in the regime of small friction, $\eta \rightarrow 0$. The two extra equations correspond to the differential (and static) form of energy-momentum conservation (6). They result from the assumption that the system is locally in equilibrium, also on scales that are comparable with the wall thickness. Their integration across the wall gives immediately Steinhardt's matching conditions (8).

In order to solve the system of equations, we proceed as follows. The basis quantity is the free energy of the system $\mathcal{F}(\phi, T)$ from which all the thermodynamic potentials can be derived. We determine the nucleation temperature of the system using the standard techniques of the bounce solution [21]. With a specific wall velocity ξ_w and this information, the hydrodynamic system (9) can be solved. Finally, we solve the system of differential equations (50)-(52) and determine which friction coefficient η corresponds to the wall velocity ξ_w we have chosen. When the wall velocity is increased, the friction coefficient eventually turns negative. This signals the occurrence of the hydrodynamic obstruction. The numerical results obtained by this procedure depend neither on the bag equation of state nor on the assumption of small fluid or wall velocities.

The system of equations can be solved in the following way: First, equation (51) can be used to obtain the fluid velocity as a function of the Higgs vev and the temperature

$$v(\phi, T) = -\frac{\omega(\phi, T)}{2\omega_+ \gamma_+^2 v_+} + \sqrt{1 + \frac{\omega(\phi, T)^2}{4\omega_+^2 \gamma_+^4 v_+^2}} . \quad (54)$$

Then eq. (52) can be used to obtain a closed expression for $\partial_z \phi(\phi, T)$

$$\frac{1}{2} (\partial_z \phi(\phi, T))^2 = \omega \gamma^2 v^2 + p - \omega_+ \gamma_+^2 v_+^2 - p_+ . \quad (55)$$

Finally, the Higgs equation (50) can be recast using (52) as

$$\partial_z \phi \frac{\partial p}{\partial \phi} - \partial_z \phi \mathcal{K} = \partial_z (\omega \gamma^2 v^2 + p) , \quad (56)$$

which leads to

$$\frac{d\phi}{dT} = \frac{\partial_T (\omega \gamma^2 v^2 + p)}{\mathcal{K} - \partial_\phi (\omega \gamma^2 v^2)} . \quad (57)$$

For a fixed wall velocity ξ_w , one unique choice of η leads to the correct boundary conditions $\phi(T_{\pm}) = \phi_{\pm}$. The wall velocity can then be varied to lead to the velocity corresponding to the obstruction where $\eta = 0$.

As a remark we note that solving the system of local equations (52) also allows to determine the wall thickness. Usually the wall thickness is determined for the nucleated bubbles from the bounce solution. In principle the wall thickness during the bubble expansion is expected to be smaller than this value since the acceleration of the wall also compresses the wall. In practice we find that this effect changes the wall thickness by only a few percent.

4.2 A concrete (toy) model

Consider the effective potential

$$V(\phi, T) = \lambda(\phi^2 - v^2)^2 - \frac{a_+}{3} T^4 + c_1 T^2 \phi^2 - c_2 T \phi^3 . \quad (58)$$

This model is inspired by systems where the strength of the phase transition comes from thermal contributions of bosons coupled to the Higgs that add to the thermal potential terms proportional to $T\phi^3$. This is for example the case in the light stop scenario [24] of the MSSM where the W-bosons and the stops give rise to the cubic terms. Another example of this class of models are hidden sector models [25]. The parameters λ , c_1 and c_2 can be exchanged for the Higgs mass m_H , the critical temperature T_c and the ratio ϕ_c/T_c according to

$$m_H^2 = 8\lambda v^2, \quad \frac{\phi_c}{T_c} = \frac{c_2}{2\lambda}, \quad T_c = \frac{4\lambda v}{\sqrt{8c_1\lambda - 2c_2^2}} . \quad (59)$$

The latent heat ℓ_c is given by

$$\ell_c \simeq T \partial_T [V(T, \phi_c) - V(T, 0)]_{T=T_c} = 4\lambda\phi_c^2 v^2 , \quad (60)$$

and hence

$$\alpha_c = \frac{\lambda\phi_c^2 v^2}{a_+ T_c^4} . \quad (61)$$

The nucleation temperature can be determined using the expression for the tunneling action in the thin-wall approximation

$$S_3/T = \sqrt{2} \frac{4\pi}{81} \frac{\lambda^{3/2} \phi_c^9}{\ell_c^2 T_N} \left(1 - \frac{T}{T_c}\right)^{-2} , \quad (62)$$

yielding for the nucleation temperature ($S_3/T_N \approx 140$)

$$\log \frac{T_c}{T_N} \simeq \left(1 - \frac{T_N}{T_c}\right) \simeq 0.04 \frac{\lambda^{3/4} \phi_c^4}{\ell_c} \sqrt{\frac{\phi_c}{T_c}} . \quad (63)$$

Using this in (40) one obtains

$$\xi_w^2 \in (0.7 \div 1.4) \left(\frac{g_*}{100}\right) \left(\frac{v}{m_H}\right)^{5/2} \left(\frac{T_c}{v}\right)^4 \sqrt{\frac{\phi_c}{T_c}} , \quad (64)$$

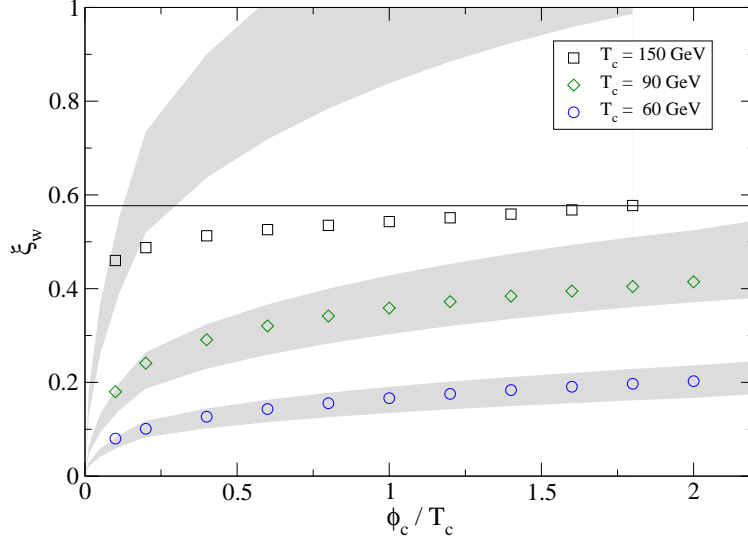


Figure 3: The wall velocity of the obstruction versus ϕ_c/T_c for the values $T_c = 0.6$, $T_c = 0.9$, and $T_c = 1.5$. The Higgs mass is $m_H = 120$ GeV and the gray bands correspond to the estimate in (40).

where the number of degrees of freedom in the symmetric phase g_* is given by $g_* = 30 a_+/\pi^2$. Hence the obstruction velocity depends in the regime of weak phase transitions only weakly on ϕ_c . Still, the thin-wall approximation (62) is not very accurate and we use numerical results for the nucleation temperature in the following.

The result from solving the local equations compared to the estimate in (40) is shown in Fig. 3. As expected, for small velocities the estimate works rather well while it underestimates the heating effect in front of the wall when the wall velocity approaches the speed of sound.

In the last section we found the criterion (48) for the occurrence of the obstruction under the assumption that the temperature in front of the wall equals the average one. In the following we discuss how this criterion is modified if this assumption is replaced by the local system of equations. Still, one would like to express the criterion for the occurrence of the obstruction in terms of critical and nucleation temperature only, since these quantities can be obtained by inspecting the effective potential without an hydrodynamic analysis of the deflagration mode. Especially for weak phase transitions one would expect that the criterion (48) is only modified by a proportionality factor $c(\alpha_c)$ close to unity:

$$\log \frac{T_c}{T_N} < c(\alpha_c)\Omega(\alpha_c) . \quad (65)$$

In order to test this hypothesis, we determine the wall velocity of the obstruction in the model (58). We keep α_c fixed and vary T_c in such a way that $\xi_w = c_s$. The functions $\log \frac{T_+}{T_N} = \Omega(\alpha_+)$, $\log \frac{T_c}{T_N}$ and $\Omega(\alpha_c)$ are plotted in the right panel of Fig. 4. It turns out that the proportionality factor in (65) is for small α_c close to $\frac{3}{4}$. This factor depends in principle on the model but it is expected to be in the range $[\frac{1}{2}, 1]$. The upper bound results from the fact that the average temperature in the wall cannot exceed T_+ . The lower bound is due to the fact that the average temperature cannot fall below T_- and that for small α_c the heating effect is behind the wall half as strong as in front (see eqs. (35) and (39)). Still, there is a

certain uncertainty in this factor².

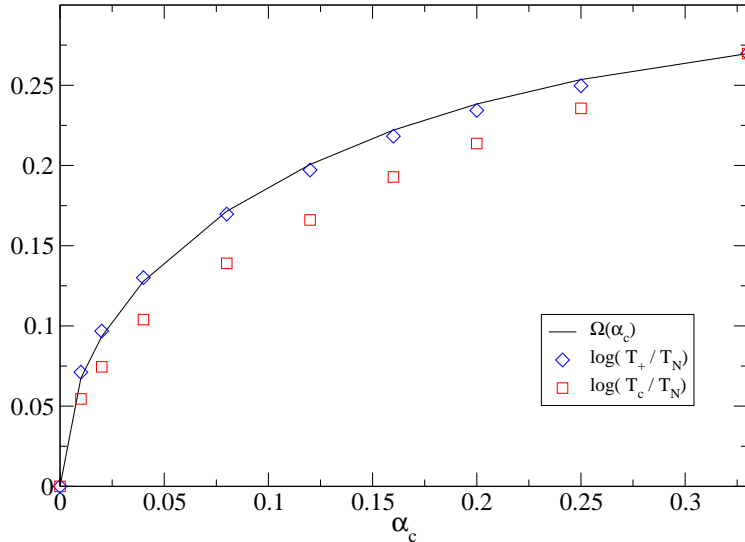


Figure 4: The heating effect assuming a wall velocity of the speed of sound, $\xi_w = c_s$. The plot displays the relation between the parameters of the phase transition at critical temperature in relation to the parameters in front of the phase boundary in the toy model (58).

Interestingly, the criterion (48) becomes exact in the limit $\alpha_c \rightarrow 1/3$. This can be explained by noting that in the limit $\alpha_c \rightarrow 1/3$, the velocity in front of the wall equals the bubble wall velocity, $v_+ = 0$, and so the temperature behind the wall T_- has to drop to zero. Thus, the combination $\omega\gamma^2v$ is constant in the wall and small. According to (57) this implies

$$\frac{d\phi}{dT} \simeq -\frac{1}{\omega\gamma^2v} \frac{\partial_T p}{\partial_\phi v}, \quad (66)$$

and therefore the Higgs vev changes quickly close to the broken phase (where v is small) and slowly close to the symmetric phase (where p is small). Hence in this limit one obtains $T_+ \rightarrow T_c$ and the criterion (48) becomes exact. However, this behavior could result from the assumption of local equilibrium and might not be reproduced if the full set of Boltzmann equations are solved instead.

5 Friction revisited

The analysis in the last few sections dealt with the hydrodynamic obstruction in the limit of vanishing friction what gives an upper limit on the wall velocity. In this section we indicate how both effects - heating and friction - can be taken into account.

Our starting point is again the equation of motion of the Higgs field (12)

$$\square\phi + \frac{\partial\mathcal{F}}{\partial\phi} - \mathcal{K}(\phi) = 0. \quad (67)$$

²For a model with an additional ϕ^6 term in the Higgs potential the proportionality factor also turns out to be close to $\frac{3}{4}$ similar to the toy model of weak phase transitions.

where $\mathcal{F}(\phi, T)$ denotes the free energy of the system and $\mathcal{K}(\phi)$ quantifies non-equilibrium effects that ultimately lead to friction and hinder the bubble expansion. Integration of the equation determines the acceleration rate of the bubble wall, which is of the form

$$\dot{\xi}_w \propto (\mathcal{F}_- - \mathcal{F}_+) (\bar{T}) - \xi_w \eta , \quad (68)$$

where \mathcal{F}_\pm are the free energies in the symmetric and broken phase, and the coefficient η parametrizes the friction. The temperature \bar{T} should be identified with the average temperature in the wall, that can differ significantly from T_N due to the compression wave in front of the bubble wall in the deflagration mode. Taking this effect into account leads (for small wall velocities ξ_w) to an equation of the form

$$\dot{\xi}_w \propto (\mathcal{F}_- - \mathcal{F}_+) (T_N) - \xi_w^2 \kappa - \xi_w \eta , \quad (69)$$

where κ is (for small α_c) approximately given by

$$\kappa = \xi_w^{-2} \left(1 - \frac{T_N}{\bar{T}} \right) T_c \left. \frac{\partial (\mathcal{F}_- - \mathcal{F}_+)}{\partial T} \right|_{T=T_c} \simeq \xi_w^{-2} \left(1 - \frac{T_N}{\bar{T}} \right) \ell_c \simeq 4\alpha_c \ell_c . \quad (70)$$

This equation is only valid for weak phase transitions ($\alpha_c \ll 1$) and small wall velocities ($\xi_w \ll 1$) but a generalization can be easily obtained by solving the hydrodynamic system along the lines of sec. 3 in other regimes. For models where the friction coefficient η is known (in particular for models with a particle content similar to the SM or MSSM), this approach can be used to obtain accurate wall velocities.

6 Discussion

We discussed the expansion velocity of nucleated bubbles in a first-order phase transition. For the subsonic deflagration mode, the expansion is not only hindered by friction (that results from deviations from equilibrium) but also due to a heating effect by the compression wave in front of the bubble wall. Even if friction is neglected, the heating effect by itself can lead to an upper limit on the expansion velocity of the bubbles.

In summary, a criterion for the occurrence of these obstructions at subsonic wall velocities is given by

$$\log \frac{T_c}{T_N} < c(\alpha_c) \Omega(\alpha_c) , \quad (71)$$

where T_c and T_N denote the critical and nucleation temperature of the phase transition, respectively. The parameter α_c quantifies the strength of the phase transition and is given by $\alpha_c = \frac{\ell_c}{4e_c}$ where ℓ_c denotes the latent heat and e_c the energy density of the plasma in the symmetric phase, both evaluated at the critical temperature. A fit to the model-independent function $\Omega(\alpha_c)$ is given in eq. (47). Finally, the function $c(\alpha_c)$ is a model-dependent fudge factor that approaches unity for $\alpha_c \rightarrow \frac{1}{3}$ and a constant in the range $[\frac{1}{2}, 1]$ in the limit $\alpha_c \rightarrow 0$. For the model of weak phase transitions given in (58) as well as the SM with an additional ϕ^6 term in the Higgs potential it is found to be close to $\frac{3}{4}$.

Let us discuss this result in the context of different models. Consider the MSSM in the light stop scenario [24, 26]. Using the characteristics of the phase transition

$$\phi_c \simeq T_c \simeq 95 \text{ GeV}, \quad m_H \simeq 120 \text{ GeV} , \quad (72)$$

in (61) and (63) leads to

$$\alpha_c = 2.6 \times 10^{-2}, \quad \log \frac{T_c}{T_n} = 3.4 \times 10^{-3}, \quad (73)$$

and an obstruction at the velocity $\xi_w \simeq 0.18$. Hence, one can conclude even without the knowledge of the friction coefficient that the wall velocity in the MSSM is subsonic what is a necessary requirement for electroweak baryogenesis. An analysis of friction without the heating effect [11] leads to a wall velocity $\xi_w \simeq (0.05 \div 0.1)$ what shows that in this model friction is very relevant.

Next consider the SM with the (unrealistic) parameters

$$\phi_c \simeq 60 \text{ GeV}, \quad T_c \simeq 120 \text{ GeV}, \quad m_H \simeq 90 \text{ GeV}, \quad (74)$$

what corresponds to one parameter set in ref. [10] and yields

$$\alpha_c = 2.3 \times 10^{-3}, \quad \log \frac{T_c}{T_n} = 1.1 \times 10^{-3}, \quad (75)$$

and hence $\xi_w \simeq 0.35$. In comparison, in [10] the heating effect as well as friction was taken into account and a wall velocity in the range $\xi_w \in [0.35, 0.40]$ was found. The result was not very sensitive towards changes in the interaction rates such that the heating in front of the phase boundary is the dominant effect hindering the wall expansion. This also fits well with the results in [27] that neglected the heating effect and found much larger wall velocities.

Let us discuss some cases where the wall velocity is still unknown. Consider the nMSSM as discussed in [28, 29]. In this model, typical parameters for a phase transition that is on the strong end of the spectrum are³

$$T_c \simeq 75 \text{ GeV}, \quad T_n \simeq 65 \text{ GeV}, \quad \alpha_c \simeq 8.9 \times 10^{-2}, \quad (76)$$

what leads to a subsonic wall velocity according to (71) and electroweak baryogenesis is feasible in this model.

Finally, consider the SM enhanced by a large number of singlets from a hidden sector as discussed in [25]. For a singlet coupling to the Higgs of order $\zeta \simeq 1.0$ and a Higgs mass $m_H = 125 \text{ GeV}$ one finds for example the following characteristics of the phase transition⁴

$$T_c \simeq 100 \text{ GeV}, \quad T_n \simeq 93 \text{ GeV}, \quad \alpha_c \simeq 1.9 \times 10^{-2}, \quad (77)$$

and hence a wall velocity $\xi_w \simeq c_s$ [using the criterion for large velocities (71)]. For smaller values of the scalar self-coupling ζ and/or larger Higgs masses the phase transition becomes weaker such that for these parameters the wall velocity is definitely subsonic. On the other hand, under the assumption that the friction is similar to the SM, the wall velocity is supersonic for larger values of ζ and/or smaller Higgs masses and can even enter the runaway regime according to the analysis in ref. [14].

³Notice that in [28, 29] the latent heat normalized to the energy density at the nucleation temperature is denoted α .

⁴Also in [25] the latent heat normalized to the energy density at the nucleation temperature is denoted α .

Acknowledgment

We are grateful to Geraldine Servant for helpful comments on the manuscript. T.K. acknowledges support from the European Commission the European Research Council Starting Grant Cosmo@LHC. The work of J.M.N. was partially supported by the European Community under the contract PITN-GA-2009-237920 and by the Agence Nationale de la Recherche.

References

- [1] A. G. Cohen, D. B. Kaplan and A. E. Nelson, Phys. Lett. B **245** (1990) 561; Nucl. Phys. B **349** (1991) 727; Nucl. Phys. B **373** (1992) 453; Phys. Lett. B **336** (1994) 41 [hep-ph/9406345]. For a review see e.g J. M. Cline, [hep-ph/0609145].
- [2] E. Witten, Phys. Rev. D **30**, 272 (1984).
- [3] A. Kosowsky, M. S. Turner and R. Watkins, Phys. Rev. D **45** (1992) 4514; Phys. Rev. Lett. **69**, 2026 (1992); A. Kosowsky and M. S. Turner, Phys. Rev. D **47** (1993) 4372 [astro-ph/9211004].
- [4] M. Kamionkowski, A. Kosowsky and M. S. Turner, Phys. Rev. D **49** (1994) 2837 [astro-ph/9310044].
- [5] C. Caprini, R. Durrer and G. Servant, Phys. Rev. D **77** (2008) 124015 [astro-ph/0711.2593];
- [6] S. J. Huber and T. Konstandin, JCAP **0809** (2008) 022 [hep-ph/0806.1828];
- [7] C. Caprini, R. Durrer, T. Konstandin and G. Servant, [astro-ph/0901.1661].
- [8] A. Kosowsky, A. Mack and T. Kahniashvili, Phys. Rev. D **66** (2002) 024030 [astro-ph/0111483]; A. D. Dolgov, D. Grasso and A. Nicolis, Phys. Rev. D **66** (2002) 103505 [astro-ph/0206461]; G. Gogoberidze, T. Kahniashvili and A. Kosowsky, Phys. Rev. D **76** (2007) 083002 [astro-ph/0705.1733].
- [9] C. Caprini and R. Durrer, Phys. Rev. D **74** (2006) 063521 [astro-ph/0603476]; C. Caprini, R. Durrer and G. Servant, JCAP **0912** (2009) 024 [astro-ph.CO:0909.0622].
- [10] G. D. Moore and T. Prokopec, Phys. Rev. D **52** (1995) 7182 [hep-ph/9506475].
- [11] P. John and M. G. Schmidt, Nucl. Phys. B **598** (2001) 291 [Erratum-ibid. B **648** (2003) 449] [hep-ph/0002050].
- [12] D. Bodeker and G. D. Moore, JCAP **0905** (2009) 009 [hep-ph/0903.4099].
- [13] H. Kurki-Suonio and M. Laine, Phys. Rev. Lett. **77** (1996) 3951 [arXiv:hep-ph/9607382].
- [14] J. R. Espinosa, T. Konstandin, J. M. No and G. Servant, JCAP **1006** (2010) 028 [arXiv:1004.4187 [hep-ph]].

- [15] M. S. Carena, J. M. Moreno, M. Quiros, M. Seco and C. E. M. Wagner, Nucl. Phys. B **599** (2001) 158 [arXiv:hep-ph/0011055].
- [16] S. J. Huber, P. John and M. G. Schmidt, Eur. Phys. J. C **20** (2001) 695 [arXiv:hep-ph/0101249].
- [17] L. D. Landau and E. M. Lifshitz, “Fluid Mechanics,” Pergamon Press, New York, 1989.
- [18] P. J. Steinhardt, Phys. Rev. D **25** (1982) 2074.
- [19] H. Kurki-Suonio, Nucl. Phys. B **255** (1985) 231. M. Gyulassy, K. Kajantie, H. Kurki-Suonio and L. D. McLerran, Nucl. Phys. B **237**, 477 (1984); K. Kajantie and H. Kurki-Suonio, Phys. Rev. D **34**, 1719 (1986); K. Enqvist, J. Ignatius, K. Kajantie and K. Rummukainen, Phys. Rev. D **45** (1992) 3415; M. Dine, R. G. Leigh, P. Y. Huet, A. D. Linde and D. A. Linde, Phys. Rev. D **46** (1992) 550 [hep-ph/9203203]; B. H. Liu, L. D. McLerran and N. Turok, Phys. Rev. D **46** (1992) 2668; P. Y. Huet, K. Kajantie, R. G. Leigh, B. H. Liu and L. D. McLerran, Phys. Rev. D **48** (1993) 2477 [hep-ph/9212224]; J. Ignatius, K. Kajantie, H. Kurki-Suonio and M. Laine, Phys. Rev. D **49** (1994) 3854 [astro-ph/9309059]. M. Laine, Phys. Rev. D **49** (1994) 3847 [hep-ph/9309242]. J. C. Miller and L. Rezzolla, Phys. Rev. D **51** (1995) 4017 [astro-ph/9411091]. H. Kurki-Suonio and M. Laine, Phys. Rev. D **51**, 5431 (1995) [hep-ph/9501216].
- [20] L. Leitaο and A. Megevand, arXiv:1010.2134 [astro-ph.CO].
- [21] C. G. Callan and S. R. Coleman, Phys. Rev. D **16**, 1762 (1977). S. R. Coleman, Phys. Rev. D **15**, 2929 (1977) [Erratum-ibid. D **16**, 1248 (1977)]. A. D. Linde, Phys. Lett. B **100**, 37 (1981).
- [22] H. Kurki-Suonio and M. Laine, Phys. Rev. D **51** (1995) 5431 [arXiv:hep-ph/9501216].
- [23] A. Megevand and A. D. Sanchez, [hep-ph/0904.1753]; Nucl. Phys. B **825** (2010) 151 [hep-ph/0908.3663].
- [24] M. S. Carena, M. Quiros and C. E. M. Wagner, Phys. Lett. B **380**, 81 (1996) [arXiv:hep-ph/9603420].
- [25] J. R. Espinosa, T. Konstandin, J. M. No and M. Quiros, Phys. Rev. D **78**, 123528 (2008) [arXiv:0809.3215 [hep-ph]].
- [26] J. M. Moreno, M. Quiros and M. Seco, Nucl. Phys. B **526** (1998) 489 [arXiv:hep-ph/9801272].
- [27] G. D. Moore and T. Prokopec, Phys. Rev. Lett. **75**, 777 (1995) [arXiv:hep-ph/9503296].
- [28] R. Apreda, M. Maggiore, A. Nicolis *et al.*, Nucl. Phys. **B631** (2002) 342-368. [gr-qc/0107033].
- [29] S. J. Huber, T. Konstandin, T. Prokopec and M. G. Schmidt, Nucl. Phys. B **757**, 172 (2006) [arXiv:hep-ph/0606298].